

Toward a Unified Picture of the Water Self-Ions at the Air–Water Interface: A Density Functional Theory Perspective

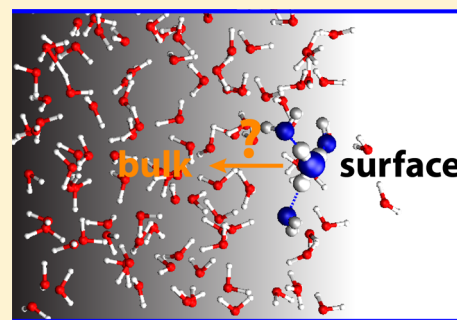
Marcel D. Baer,[†] I-Feng W. Kuo,[‡] Douglas J. Tobias,[§] and Christopher J. Mundy^{*,†}

[†]Physical Science Division, Pacific Northwest National Laboratory, Richland, Washington 99352, United States

[‡]Chemical Sciences Division, Lawrence Livermore National Laboratory, Livermore, California 94550, United States

[§]Department of Chemistry, University of California, Irvine, California 92697-2025, United States

ABSTRACT: The propensities of the water self-ions, H_3O^+ and OH^- , for the air–water interface have implications for interfacial acid–base chemistry. Despite numerous experimental and computational studies, no consensus has been reached on the question of whether or not H_3O^+ and/or OH^- prefer to be at the water surface or in the bulk. Here we report a molecular dynamics simulation study of the bulk vs interfacial behavior of H_3O^+ and OH^- that employs forces derived from density functional theory with a generalized gradient approximation exchange–correlation functional (specifically, BLYP) and empirical dispersion corrections. We computed the potential of mean force (PMF) for H_3O^+ as a function of the position of the ion in the vicinity of an air–water interface. The PMF suggests that H_3O^+ has equal propensity for the interface and the bulk. We compare the PMF for H_3O^+ to our previously computed PMF for OH^- adsorption, which contains a shallow minimum at the interface, and we explore how differences in solvation of each ion at the interface vs in the bulk are connected with interfacial propensity. We find that the solvation shell of H_3O^+ is only slightly dependent on its position in the water slab, while OH^- partially desolvates as it approaches the interface, and we examine how this difference in solvation behavior is manifested in the electronic structure and chemistry of the two ions.



■ INTRODUCTION

One of the fundamental chemical processes that occurs in aqueous solution is the autodissociation of water, which produces the so-called water self-ions, hydrated protons and hydroxide anions. Acid–base chemistry at aqueous interfaces is important in a wide variety of systems in biology, the environment, and materials science. Thus, the propensity of the water self-ions for aqueous interfaces is a subject of fundamental interest that has potentially widespread implications. Accordingly, this subject has received a great deal of attention during the past few years. Unfortunately, despite the large number of studies employing a broad array of experimental and theoretical/computational techniques, no clear consensus has yet emerged on the question of whether or not the interfacial population of the water ions is enhanced or depleted with respect to their bulk populations (for recent reviews and commentaries, see refs 1–6).

On the experimental side, there is evidence from thermodynamic (e.g., surface tension) and spectroscopic data for modest enhancement of the interfacial population of excess protons and repulsion of hydroxide anions at aqueous–air interfaces. The surface tensions of aqueous solutions of strong acids decrease as a function of concentration, whereas the surface tension increments for strong bases are positive, and resemble those of inorganic salts.⁷ According to the Gibbs adsorption equation,⁸ the negative surface tension increments of the acids imply that the surface excesses of the acid dissociation products (protons and counterions) are positive,

and the positive surface tension increments of the bases imply that the surface excesses of the base dissociation products (hydroxide anions and counterions) are negative. Thus, one interpretation of the surface tension data is that there is an enhancement of protons and depletion of hydroxide at the air–water interface. This simple interpretation is supported by a salt ion partitioning model of surface tension increments.⁹

Surface-sensitive spectroscopic experiments, including vibrational sum-frequency generation (SFG) and second harmonic generation (SHG), provide evidence for the presence of excess protons in the vicinity of the air–solution interface of acid solutions.^{2,10–14} Moreover, SHG data for strong base solutions could be interpreted in terms of a wide range of behavior, from weak hydroxide adsorption to strong hydroxide repulsion at the solution–air interface, but not in terms of strong adsorption.² Phase-sensitive SFG data on a 1.2 M NaOH solution show that OH^- is present, but not necessarily strongly enhanced, in the water hydrogen bonding network near the solution–air network.¹⁴ The lack of strong hydroxide adsorption to the water surface inferred from SHG and SFG data is supported by X-ray photoemission measurements of the surface vs bulk composition of aqueous NaOH solutions¹⁵ and SFG measure-

Special Issue: James L. Skinner Festschrift

Received: February 21, 2014

Revised: April 15, 2014

ments of the pH dependence of water orientation at oil droplet–water interfaces.¹⁶

While surface tension and surface-selective spectroscopic data on aqueous acid and base solutions are consistent with selective adsorption of protons at aqueous–nonpolar (air and oil) interfaces, other experiments have been interpreted in terms of selective adsorption of hydroxide. For example, electrokinetic measurements on gas–water and oil–water interfaces and water on neutral surfaces have been interpreted in terms of a pH-dependent negative charge with an isoelectric point of $\text{pH} \approx 4$ at aqueous interfaces, which is attributed to the adsorption of hydroxide anions.^{4,17–19} The hydroxide adsorption free energy has been estimated to be $25 k_{\text{B}}T$ from the pH dependence of the ζ potential of oil droplets in water¹⁷ and $16\text{--}20 k_{\text{B}}T$ from an analysis of the relaxation of the dynamic surface tension of the air–water interface.²⁰ These values imply a tremendous excess of hydroxide at water surfaces that is not consistent with surface tension increment data on acid and base solutions over wide concentration ranges. A strong adsorption of hydroxide anion has been invoked in a very recent analysis, based on the Gibbs adsorption equation, of the pH dependence of the surface tension of water.²¹ Electrospray mass spectrometry measurements of proton transfer reactions in aqueous microjets are consistent with an excess of hydroxide anions on the water surface down to $\text{pH} \approx 4$.^{22,23}

The strong surface preference of hydroxide inferred from some experiments is in stark contrast to the weak surface preference of protons and weak to modest repulsion of hydroxide from water surfaces inferred from other experiments. Computational results have exhibited less variability, but a consensus on the interfacial preferences of the water ions has still not been reached in the computer simulation community. Several models have been developed to study the propensity of excess protons for the air–water interface using molecular dynamics (MD) simulations. The proton has been modeled as a single molecular species (e.g., hydronium or H_3O^+) or an excess proton that can form a variety of complexes with water (e.g., H_3O^+ , H_5O_2^+ , H_9O_4^+ , etc.). The former has been modeled primarily using polarizable force fields,^{1,10,24–30} whereas the latter has been almost exclusively modeled using multistate empirical valence bond (MS-EVB) methods that can account for the hopping of the proton defect through both the “Eigen” (H_3O^+ , H_9O_4^+) and “Zundel” (H_5O_2^+) species.^{31–39} Using the MS-EVB approach, the Voth group was the first to demonstrate the propensity of the excess proton for an extended air–water interface.³¹ In a subsequent study, they suggested that it was the amphiphilic nature of the Eigen form that produces a minimum in the potential of mean force (PMF) consistent with an interfacial propensity of $\sim 2 \text{ kcal}\cdot\text{mol}^{-1}$.³⁵ Moreover, amphiphilicity has been implicated in the pairing of hydronium ions in concentrated acid solutions.^{33,34,40} In a more recent study, Voth and co-workers attributed the enthalpic stabilization of the excess proton at hydrophobic interfaces to the displacement of unfavorable interfacial water molecules, which more than compensates the energetic penalty resulting from the loss of coordinating water molecules.⁴¹ Strong proton adsorption was also predicted using another nonpolarizable MS-EVB model,³⁹ but yet another recently developed MS-EVB model that explicitly accounts for electronic polarization predicted no surface preference for the proton.³⁷

A strongly adsorbing hydronium ion is also supported by a polarizable anion dielectric continuum theory (PA-DCT) calculation, in which the hydronium ion is modeled as a

point defect with an interaction with the interface modeled as an attractive square well potential when the proton is on the order of a hydrogen bond length from the air–water interface.⁴² The depth of the square well is the only adjustable parameter of the theory, and a value of $-1.8 \text{ kcal}\cdot\text{mol}^{-1}$ provided an excellent fit of the experimental surface tension data for HCl over a range of concentrations from 0 to 1 M. This value of the well depth is in good agreement with PMFs for proton absorption obtained from MS-EVB models,^{35,39,41} and the same value can recapitulate well the experimental surface tensions of other hydrohalous acids.⁴²

A somewhat different picture emerges from the majority of simulation studies that used empirical potentials for H_3O^+ . An early study by Dang and co-workers reported a PMF for H_3O^+ adsorption which suggested that the hydronium cation is neither strongly attracted to nor repelled from the air–water interface, in contrast to the aforementioned MS-EVB simulations and PA-DCT calculations.^{24,43} Other force fields predict a strong preference of H_3O^+ for the interface.^{1,25,30} A recent investigation highlighted the sensitivity of H_3O^+ adsorption to the details of the parametrization of the force field.²⁷ Specifically, it was shown that when the hydronium parameters are tuned so that its O atom has the ability to accept a weak hydrogen bond from water, in agreement with high level quantum chemical calculations on microsolvated H_3O^+ , the resulting PMF predicts equal likelihood for the Eigen species to be in the bulk or at the air–water interface.²⁷ This study brings into full relief the importance of a single, weak hydrogen bonding-type interaction in the classification of the hydronium ion as being either a point defect in the hydrogen bonding network of water or a distinct ion that forms a hydrophobic cavity.

The adsorption of hydroxide anions to the air–water interface has been investigated by several groups employing MD simulations with empirical force fields. The majority of these studies predict that hydroxide is repelled from the interface, and that hydroxide at the water surface is $\sim 1 \text{ kcal}\cdot\text{mol}^{-1}$ less stable than in the bulk.^{1,25,30,44} An exception is the polarizable MS-EVB model of Wick and Dang, which predicts a flat PMF for hydroxide adsorption that becomes repulsive when a Na^+ counterion is included in the calculation.^{44,45}

The variability in the extent of adsorption of the water ions predicted by force-field-based MD simulations reflects, in part, the difficulty of parametrizing models of reactive species, which is hampered by the paucity of quantitative experimental data on the composition and structure of liquid aqueous interfaces. However, because the water ions can easily change their chemical identity on short time scales, they are particularly well-suited for *ab initio* methods, which do not require a parametrization and hence, in principle, are capable of describing bulk and interfacial settings on an equal footing. The use of Kohn–Sham density functional theory (DFT) to study the complex chemistry of proton transport under bulk conditions has been thoroughly reviewed.^{46,47} On the basis of extensive comparison of DFT-based MD simulation results with a wide variety of experimental data, it appears that the best presently computationally tractable approach is to use a generalized gradient approximation (GGA) for the exchange–correlation functional.^{46,47}

Simulating the surface propensity of any ion with *ab initio* forces is subject to a variety of serious technical issues, including simulation protocols, system size, and statistical convergence of the results. In the present study, we investigate

the propensity of the water ions for the air–water interface using a DFT-based approach that has been validated by careful comparison with experimental data on the bulk solvation of atomic and molecular ions.^{48–50} The same approach can be expected to accurately describe the behavior of ions at interfaces because the solvation driving forces for ion adsorption are local.^{51,52}

The propensities of the water ions for aqueous interfaces have been investigated in several previous DFT-based simulation studies that have produced mixed results. On the one hand, Buch et al. observed that an excess proton placed initially on the surface of an 11 Å-thick water slab remained there on the time scale of a few ps, while a similarly placed hydroxide ion left the surface in less than 1 ps and remained in the interior of the slab for the duration of a few ps simulation. These observations were corroborated by longer simulations employing a thicker slab.⁵³ On the other hand, Kudin and Car found that both the excess proton and hydroxide have propensities for the interface of water with a rigid hydrophobic surface, and that hydroxide appears to interact more favorably with the surface on a time scale of 16 ps.⁵⁴ These findings were supported by DFT-based calculations of PMFs for the adsorption of hydronium and hydroxide ions to the air–water interface. In the PMF for H₃O⁺ adsorption in an 18 Å-thick water slab reported by Lee and Tuckerman, bulk and interfacial locations of the ion have essentially the same free energy, and there is an ~2 kcal·mol^{−1} barrier to adsorption in the subsurface layer.²⁶ We recently reported a PMF for OH[−] adsorption in a 31 Å-thick water slab that displayed a shallow well suggesting that OH[−] is slightly more stable at the interface than in the bulk.⁵⁵

In this paper, we report a DFT-based simulation study of the adsorption of H₃O⁺ to the air–water interface using the same protocols as in our previous investigation of the interfacial propensity of OH[−].⁵⁵ We find that the PMF for H₃O⁺ adsorption suggests that the hydronium cation is neither attracted to nor repelled from the air–water interface. In addition, we compare and contrast the bulk vs interfacial solvation of H₃O⁺ and OH[−]. We find that the solvation shell of H₃O⁺ is only slightly dependent on its position in the water slab, while OH[−] partially desolvates as it approaches the interface, and we explore how this difference in solvation behavior is manifested in the electronic structure and chemistry of the two ions.

METHODS

System Setup and Simulation Protocols. The simulations were carried out using the CP2K software suite (<http://cp2k.org>). The forces were computed via the QuickStep module, which contains an accurate and efficient implementation of density functional theory using dual basis sets of Gaussian type orbitals (TZV2P) and plane waves (expanded to $E_{\text{cut}} = 280$ Ry) for the electron density.⁵⁶ Only the valence electrons were considered explicitly, and the core electron states were represented via Goedecker–Teter–Hutter pseudopotentials.⁵⁷ The Grimme dispersion⁵⁸ correction was used in conjunction with the Becke⁵⁹ exchange and Lee–Yang–Parr correlation⁶⁰ (BLYP) functional.

The simulations consisted of one hydronium cation and 215 water molecules in a 15 Å × 15 Å × 71.44 Å box with periodic boundary conditions applied in three dimensions, resulting in a slab of aqueous solution ~31 Å thick with a nominal bulk concentration [H₃O⁺] ≈ 0.25 M, or pH ≈ 0.6. No counterions

were included in the simulation, and the net charge of the system was compensated by a neutralizing background charge. The simulations were performed in the canonical ensemble at 300 K by coupling Nosé–Hoover chain thermostats⁶¹ with characteristic frequencies of 2000 cm^{−1} to every degree of freedom. The time step of the simulations was 0.5 fs, and the wave function was minimized to a tolerance of 10^{−6} H at each step. The system size and simulation protocols have been shown to support stable air–water interfaces with the correct bulk liquid density.⁶²

Potential of Mean Force Calculation. Following our previous investigation of hydroxide adsorption,⁵⁵ we used a harmonic restraining potential, $U(z) = K_z(z - z_0)^2$, to hold the oxygen atom of the H₃O⁺ ion at a series of positions z_0 along the direction z normal to the interface, with the force constant $K_z = 0.1$ H·bohr^{−2}. The Helmholtz free energy profile (PMF) $\Delta A(z)$ was computed by integrating the z -biased average force on the z -coordinate, $\langle F(z) \rangle_{z_0}$, over 13 points each separated by 1.06 Å. Each restrained simulation was equilibrated for roughly 5–6 ps, and the subsequent 11 ps was used for analysis.

As in our previous study of the hydroxide anion, proton transfers were inhibited by restraining the coordinate $\delta = r(\text{O}^*\text{H}) - r(\text{O}'\text{H})$, where $r(\text{O}^*\text{H})$ and $r(\text{O}'\text{H})$ are the distances between the hydronium oxygen O* and the oxygen O' of the closest water molecule to the hydronium and the proton (H) shared between them, respectively, using the potential $U(\delta^2) = K_\delta[\delta^2 - (\delta^2)_0]^2$. For a solvated hydronium in the Eigen form, $\delta \approx \pm 0.3$ Å, and the Zundel state (H₅O₂⁺) where the proton is equally shared by O* and O' corresponds to $\delta = 0$ Å.⁶³ The PMF for H₃O⁺ adsorption was computed using $(\delta^2)_0 = 0.09$ Å² and $K_\delta = 0.1$ H·bohr^{−4}. We note that this is a soft restraint that permits flexibility of the hydronium O–H bonds as well as the structure of its first solvation shell. Additional simulations were carried out using umbrella sampling in conjunction with the weighted histogram analysis method (WHAM) along the δ coordinate. Here, seven windows of roughly 5 ps were run for $0.15 < \delta < 0.42$ for each z_0 of ~13 and ~14 Å, respectively. The aforementioned z_0 values correspond to the subsurface layer just below the Gibbs dividing surface defined when the density of water is ~0.5 g/cm³.

Bulk Simulations. Additional simulations of the excess proton and a negatively charged proton defect were carried out in cubic boxes containing 95 water molecules with bulk periodic boundary conditions. To examine the effects of density on the proton transfer energetics and ionic solvation, two cell sizes were used for each system. In the first, the edge length was 14.2103 Å, giving a density of 1 g·cm^{−3}, and in the second, the edge length was 14.7224 Å, giving a density of 0.9 g·cm^{−3}. The bulk simulations used the DZVP basis set optimized for the condensed phase⁶⁴ with a 400 Ry cutoff for the density and the wave function was minimized to a tolerance of 10^{−6} H. A 14 ps trajectory was generated for each bulk system following equilibration.

RESULTS AND DISCUSSION

Free Energy Profile for H₃O⁺ Adsorption at the Air–Water Interface. The PMF for adsorption of the H₃O⁺ ion is plotted along with the water density profile in Figure 1. The latter shows that the DFT method employed gives a bulk water density close to the experimental value of 1 g·cm^{−3} at $T = 300$ K and 1 atm pressure, and that the location of the interface,

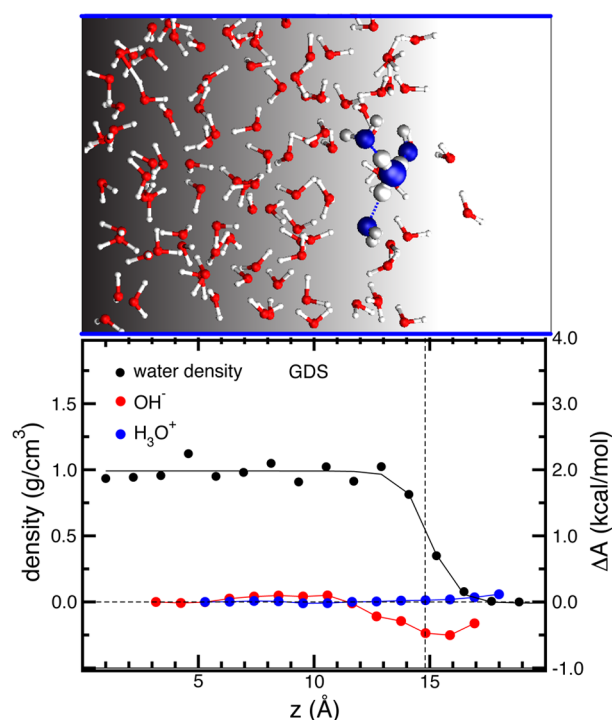


Figure 1. The upper panel shows a snapshot from an MD simulation of the hydronium ion at the air–water interface. The ion and its first solvation shell are depicted with blue and white spheres. The free energy profiles $\Delta A(z)$ for adsorption of H_3O^+ and OH^- are plotted in the lower panel using blue and red circles, respectively, and the right vertical axis. The OH^- PMF was taken from ref 55. The water density profile is plotted with filled black circles using the left vertical axis in the lower panel. The Gibbs dividing surface (GDS), determined from a fit of the density profile to a hyperbolic tangent function (black line), is indicated by the vertical dashed line at $z \approx 15$ Å.

defined here as the Gibbs dividing surface (GDS), where the water density is half its bulk value, is at $z \approx 15$ Å. The PMF is flat throughout the entire slab, and hence, we predict that the hydronium cation is neither attracted to nor repelled from the interface. Also shown in Figure 1 is the corresponding PMF for OH^- , which displays a shallow well at the GDS, with a depth of about $0.5 \text{ kcal}\cdot\text{mol}^{-1}$, suggesting that the hydroxide anion has a slight preference for the interface vs bulk.⁵⁵

However, given our limited sampling, we do not believe that the subtle differences in the PMFs for H_3O^+ and OH^- adsorption are statistically significant. A proper error analysis for the data presented in Figure 1 is difficult because the restraints on δ and z introduce long time scale (compared to the length of our trajectories) correlations in the z -component of the force on the defect oxygen atom. Moreover, the shortness of the trajectories precludes a reliable unbiasing of the restraint forces. Thus, the sub $\text{kcal}\cdot\text{mol}^{-1}$ accuracy needed to discern differences in the PMFs of the two ions cannot be statistically resolved. Nevertheless, we regard it as promising that both PMFs are flat in the bulk region, and we posit that our analysis should be sensitive to large gradients (if present) in the vicinity of the air–water interface.

The PMFs are seemingly in contradiction to what one would expect based on surface tension increments and the assumption that the counterions, say Na^+ for the hydroxide anion and Cl^- for hydronium, are both strongly repelled from the interface. At face value, it may be easy to dismiss the qualitative conclusions drawn from Figure 1 on the basis of the lack of converged

sampling that is characteristic of presently tractable DFT-based simulations. However, we will argue below that there is correlation between the details of the first solvation shell of the ions and their propensities for the air–water interface that rationalizes the PMFs.

Bulk vs Interfacial Solvation. In previous studies, it has been argued that the hydronium ion is stabilized at the air–water interface by pointing its O atom, which is a poor hydrogen bond acceptor and therefore considered hydrophobic, toward the vapor.^{33,35,40} In Figure 2, we plot

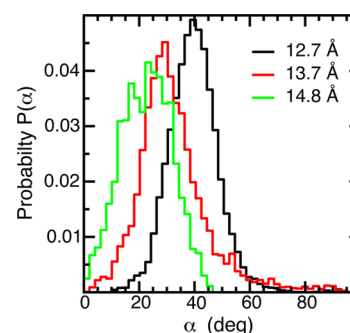


Figure 2. Orientational distributions of the hydronium ion at three locations near the air–water interface: $z = 12.7$ Å (black), 13.7 Å (red), and 14.8 Å (green); α is the angle between the normal to the interface and the molecular axis of H_3O^+ (vector pointing from the center of mass of the three hydrogen atoms to the oxygen atom). $\alpha = 0$ corresponds to the molecular axis being parallel to the surface normal.

distributions of the angle that the molecular axis of H_3O^+ makes with the surface normal. In agreement with the previous force field and DFT-based simulations, the orientational distributions from our simulations show that, as H_3O^+ approaches the interface, its molecular axis becomes more parallel to the surface normal, so that the O atom becomes more exposed to the vapor side.^{10,26,31,35}

The preferential orientation of H_3O^+ at the interface gives rise to only very subtle changes in solvation compared to the bulk. This is evident in the radial distribution functions (RDFs) and corresponding running coordination numbers (CNs) $N(r)$ plotted in Figure 3 (blue curves). The RDFs and CNs for water O atoms (O_w) around hydronium O (O^*) and H (H^*) atoms show that H_3O^+ donates three strong hydrogen bonds to water both in the bulk (Figure 3a and c) and at the interface (Figure 3d and f). In the bulk RDF for water H atoms (H_w) around the hydronium O atom, there is a small feature at $r \approx 2\text{--}2.5$ Å (inset to Figure 3b), which indicates weak hydrogen bond donation from water to the hydronium O atom, that disappears at the interface. This feature was observed in force-field-based simulation that predicted a very weak adsorption propensity for H_3O^+ .²⁷ Evidently, the weak hydrogen bond between water and the hydronium O atom plays a role in stabilizing H_3O^+ in the bulk vs the interface.

In Figure 3 (red curves), we have plotted the corresponding RDFs and CNs describing the solvation of the hydroxide anion from our earlier investigation.⁵⁵ It is readily apparent that there are significant differences in the solvation of OH^- at the interface vs in the bulk. The bulk O^*-O_w results (Figure 3a) are consistent with the “hypercoordination” of OH^- that has been observed in previous *ab initio* simulations that employed similar protocols to ours.^{46,47} A weak hydrogen bond between the hydroxide H atom and water O atoms is evident in the

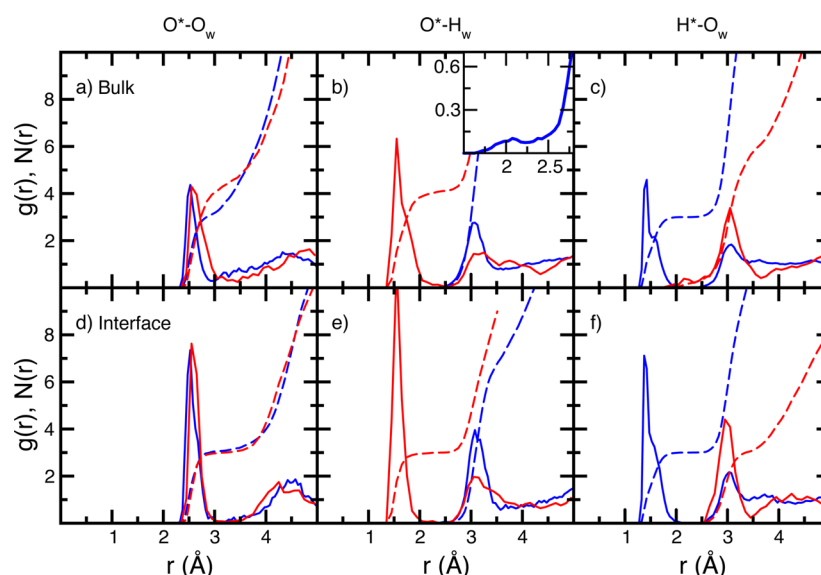


Figure 3. Blue curves: radial distribution functions $g(r)$ (solid lines) and running coordination numbers $N(r)$ (dashed lines) of water O atoms (O_w) around the hydronium O atom (O^*), water H atoms (H_w) around the hydronium O atom, and water O atoms around the hydronium H atoms (H^*). Red curves: corresponding data for the hydroxide O (O^*) and H (H^*) atoms. Panels a–c show data from the middle (bulk region) of the 215-water molecule slab, and panels d–f show data from the interface.

H^*-O_w bulk results (Figure 3c). However, at the interface, a very different picture of OH^- solvation emerges. In particular, one of the water molecules donates a hydrogen bond to the hydroxide O atom and the (partial) water molecule accepting a hydrogen bond from the hydroxide H atom departs from the solvation shell. Thus, there is a net loss of ~ 1.5 water molecules from the solvation shell, resulting in 3-fold coordination. We speculated previously that the flexibility of the hydroxide solvation shell, arising presumably from the peculiar electronic structure of OH^- , permits it to be stabilized slightly (or at least not strongly destabilized) despite being partially desolvated at the air–water interface.⁵⁵ The stability of the 3-fold coordinated hydroxide anion is supported by the structures inferred from the vibrational spectra of $OH^-(H_2O)_3$ and $OH^-(H_2O)_4$.⁶⁵

Polarization Effects in the Solvation Shells of H_3O^+ and OH^- . In the first DFT-based MD simulation of the air–water interface, it was observed that the electronic structure of undercoordinated water molecules in the vicinity of the interface is different than that of fully coordinated water molecules in the bulk.⁶⁶ For example, dipole moments of individual water molecules decreased from ~ 3 D in the bulk to ~ 2.5 D at the interface, underscoring electronic polarization effects. As can be seen in Figure 4, the average dipole moments of the water molecules in our simulations display a very similar decrease moving from the bulk to the interface.

In light of the robustness of the primarily 3-fold coordination of the hydronium ion throughout the water slab, we do not expect significant differences in the polarization of the ion and its solvation shell at the interface vs in the bulk. This is indeed the case, as can be seen in Figure 4a. Specifically, we see that, although the average dipole moment of water molecules in the first solvation shell of H_3O^+ is higher than bulk water molecules by roughly 10%, reflecting increased polarization due to interactions with the ion, it remains constant throughout the slab, even in the reduced density region of the interface ($z > 13$ Å). Likewise, the dipole moment of the hydronium ion itself does not depend on the position of the ion in the slab. Thus,

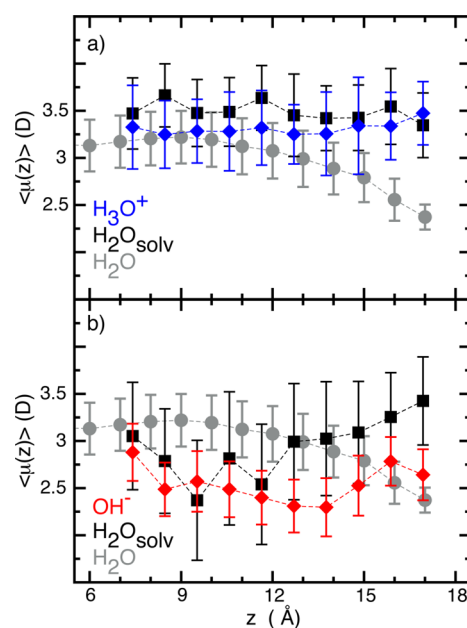


Figure 4. (a) Average dipole moment of the hydronium ion (filled blue diamonds) restrained to its bulk minimum value and water molecules in its first solvation shell (filled black squares) plotted vs position in the slab. (b) Average dipole moment of the hydroxide ion (filled red diamonds) restrained to its bulk minimum value and water molecules in its first solvation shell (filled black squares) plotted vs position in the slab. In both panels, the average dipole moment of all water molecules, symmetrized with respect to the center of the slab at $z = 0$ Å, is plotted using filled gray circles.

polarization effects do not appear to play an important role in determining the interfacial propensity (or lack thereof) of the hydronium ion. The insensitivity of the hydronium solvation shell and the electronic structure of the ion and its solvation shell to the location in the slab are consistent with the flat PMF for H_3O^+ adsorption in Figure 1.

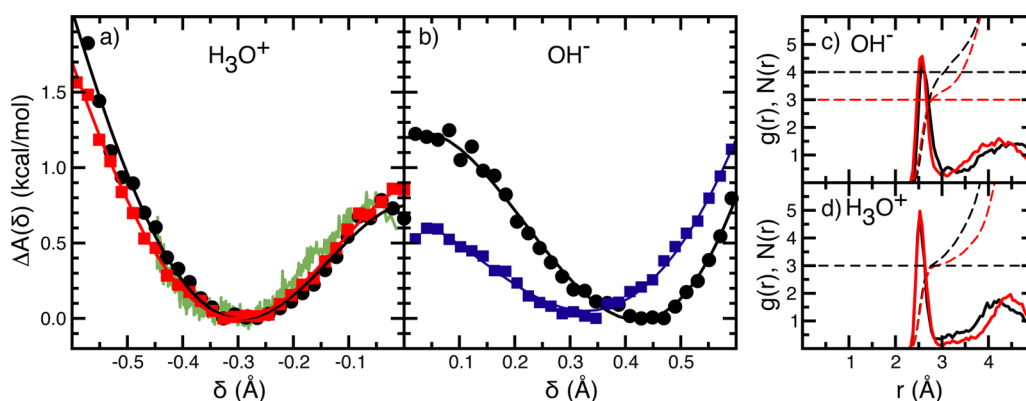


Figure 5. (a) Potentials of mean force calculated from histograms of the proton transfer coordinate δ from unrestrained simulations of an excess proton in bulk water at densities of $1.0 \text{ g}\cdot\text{cm}^{-3}$ (filled black circles) and $0.9 \text{ g}\cdot\text{cm}^{-3}$ (filled red squares). The green curve is the average potential of mean force computed by umbrella sampling along δ for two windows in the vicinity of the GDS as described in the Methods section. (b) Potentials of mean force calculated from histograms of the proton transfer coordinate δ from unrestrained simulations of a negatively charged proton defect in bulk water at densities of $1.0 \text{ g}\cdot\text{cm}^{-3}$ (filled black circles) and $0.9 \text{ g}\cdot\text{cm}^{-3}$ (filled blue squares). (c) O^*-O_w radial distribution functions $g(r)$ and running coordination numbers $N(r)$ for the hydroxide anion at $1.0 \text{ g}\cdot\text{cm}^{-3}$ (black) and $0.9 \text{ g}\cdot\text{cm}^{-3}$ (red). The horizontal dashed lines mark coordination numbers of three and four. (d) Same as c except for H_3O^+ .

The position dependence of the average dipole moment of the hydroxide anion and its solvation shell is shown in Figure 4b. The dipole moment of the ion is essentially constant, and the average dipole moment of the solvation shell appears to increase slightly as the ion is moved from the bulk to the interface. The subtle change in the dipole moment of water molecules in the solvating water molecules is presumably connected with the change from the looser (4 + 1) coordination in the bulk to the tighter 3-fold coordination at the interface. It is conceivable that the increased polarization of the solvation shell could help stabilize (or at least not destabilize) the hydroxide anion at the interface vs in the bulk.

While the pioneering MS-EVB models of Voth and co-workers predict that the excess proton has a strong interfacial propensity,^{31,35} a more recent MS-EVB model that includes electronic polarization explicitly gives a flat PMF for H_3O^+ adsorption.⁴⁴ The lack of interfacial preference for the new model was tied to the delocalization of charge into the first solvation shell of the solvated hydronium ion as it was moved toward the interface.³⁷ We looked for delocalization of the charge of the hydronium and hydroxide defects by integrating the charge density radially from the oxygen atom for the same configurations used in Figure 4 until a value of +1 or −1, respectively, was obtained.⁵⁰ We found no evidence of further charge delocalization at the interface vs in the bulk and leave a more detailed analysis of charge delocalization for a future study.

Effect of Water Density on the Solvation and Chemistry of Excess Protons and Negatively Charged Proton Defects in Bulk Water. While it is conceivable that the increased polarization of the solvation shell could help stabilize the hydroxide anion at the interface vs in the bulk, the small interfacial minimum in the free energy of adsorption does not seem to be consistent with the loss of water molecules from the solvation shell as the ion approaches the interface. Indeed, the intuitive explanation for the repulsion of a fluoride anion at the air–water interface is that strongly hydrated ions do not give up water molecules without a large enthalpic penalty. The comparison of hydroxide to fluoride seems relevant based on size and charge; namely, the bulk $\text{F}^- - \text{O}_w$ RDF is similar to the bulk hydroxide $\text{O}^* - \text{O}_w$ RDF in terms of distance of water

molecules to the ion.^{50,55,67} However, significant differences in the solvation of F^- and OH^- are observed in DFT-based MD simulations. For example, F^- has a 4-fold coordinated solvation shell in the bulk that persists as the ion is moved to the air–water interface,^{50,67,68} while OH^- has an asymmetric (4 + 1) coordinated solvation shell in the bulk that changes to 3-fold coordination at the interface (Figure 3).⁵⁵

The “flexibility” of the OH^- solvation shell is underscored by examining its behavior in the bulk as the density of the solution is reduced. With the simulation protocols employed in the present study, which include an empirical dispersion correction, the bulk water density in a system with an open interface (e.g., a slab) is close to the expected value of $1.0 \text{ g}\cdot\text{cm}^{-3}$ at 300 K and 1 atm (e.g., see Figure 1). Without the dispersion correction, the bulk water density is $\sim 0.8 \text{ g}\cdot\text{cm}^{-3}$ under the same conditions.^{62,66,67} We showed previously that OH^- exhibits 3-fold coordination in the bulk region of a water slab that was simulated without the dispersion correction, where the bulk density was $\sim 0.8 \text{ g}\cdot\text{cm}^{-3}$.⁶² To further investigate the density dependence of OH^- solvation, we performed two additional simulations, in which dispersion corrections were included, of a single hydroxide anion in a cubic box of 95 water molecules at densities of 0.9 and $1 \text{ g}\cdot\text{cm}^{-3}$. The RDFs and CNs plotted in Figure 5c show that the number of water molecules in the first solvation shell drops to three as the density is lowered to $0.9 \text{ g}\cdot\text{cm}^{-3}$, in agreement with our previous results from slab simulations.⁶² In contrast, it is evident from Figure 5d that the same reduction in density does not alter the 3-fold coordination of H_3O^+ . Returning to the comparison of F^- and OH^- , an additional difference between their solvation is that a reduction of water density (e.g., in DFT-based MD simulations without dispersion corrections) does not change the 4-fold coordination of F^- observed at normal density.^{50,67}

PMFs along the proton transfer coordinate δ for an excess proton at normal and reduced density are plotted in Figure 5a. The positions of the minima at $\delta \approx -0.3$, corresponding to the H_3O^+ species, and the height of the barriers at $\delta = 0$ corresponding to H_5O_2^+ are essentially identical. Thus, the chemistry of the excess proton is not altered when the density is lowered from 1.0 to $0.9 \text{ g}\cdot\text{cm}^{-3}$. As is evident in Figure 5b, the situation is markedly different for the negatively charged

proton defect. At $1.0 \text{ g}\cdot\text{cm}^{-3}$, the minimum corresponding to OH^- is at $\delta \approx 0.45$ and the barrier at $\delta = 0$ corresponding to H_3O_2^- is $1.2 \text{ kcal}\cdot\text{mol}^{-1}$, whereas at $0.9 \text{ g}\cdot\text{cm}^{-3}$ the minimum is at $\delta \approx 0.35$ and the barrier is $0.6 \text{ kcal}\cdot\text{mol}^{-1}$. The low density bulk proton transfer PMF for the negatively charged defect is remarkably similar to that computed at the air–water interface.⁵⁵ Thus, the tendency of OH^- to become more delocalized (lower δ) and reduce its solvation shell to 3-fold coordination at the air–water interface can be attributed to the reduced density in the vicinity of the interface.

Comparison of our results to those from a recent force-field-based study of OH^- adsorption to the air–water interface underscores the sensitivity of the PMF for adsorption to flexibility of the OH^- solvation shell. The force field, which produces a high population of $(4 + 1)$ coordinated OH^- in the bulk, significantly higher than what is observed in DFT-based simulations, and almost no 3-fold coordinated OH^- , produced a PMF in which there is an $\sim 1 \text{ kcal}\cdot\text{mol}^{-1}$ penalty for OH^- to adsorb to the surface of a 215-water-molecule droplet and a water slab.³⁰

Subtle features of the solvation of H_3O^+ may affect its PMF for adsorption to the air–water interface. On the one hand, models in which the hydronium O atom is “hydrophobic” predict strong H_3O^+ adsorption.^{31,35} On the other hand, introducing a weak interaction between the hydronium O atom and water H atoms, such as the one observed in our DFT-based simulations (see inset of Figure 3b), gives rise to a flat PMF.²⁷

CONCLUSIONS AND OUTLOOK

We have presented a unified view of the adsorption of the water self-ions H_3O^+ and OH^- to the air–water interface, according to which neither of the ions has a significant preference for or aversion to the interface. This view was developed on the basis of both the PMFs for ion adsorption and in depth structural analysis of simulations that employed DFT-based forces that naturally describe electronic structure and chemistry. Our analysis suggests a picture where both the solvation and polarization of H_3O^+ do not vary significantly as the GDS is approached. This is in contrast to OH^- where the solvation changes from a primarily $(4 + 1)$ hypercoordinated complex in the bulk to a 3-fold coordinated species and the water molecules in the hydration shell become more polarized in the vicinity of the air–water interface. The robustness of the H_3O^+ solvation shell and the flexibility of the OH^- solvation shell as a function of the location in a water slab were verified by bulk simulations of the two ions at normal and reduced water densities.

Our results are not compatible with the strong propensity of OH^- for aqueous interfaces that has been inferred from electrokinetic data.^{4,17–19} The lack of strong hydroxide adsorption predicted by our calculations is qualitatively consistent with previous simulation studies, but upon closer inspection, our results contradict the majority of force-field-based simulation studies that predict that protons preferentially adsorb to^{1,10,25,30,31,35,39} and hydroxide anions are repelled from^{1,10,15,25,44} air–water interfaces. There are, however, some force fields that produce PMFs for water ion adsorption that are similar to ours.^{24,27,37,44} The variability of force-field-based simulation results highlights the challenges of parametrizing force fields to properly describe the subtle changes in solvation and electronic structure that accompany ion adsorption, given the lack of quantitative experimental data on the structural and energetic changes that occur during the adsorption process.

Although the DFT-based approaches employed herein may be considered “model-free”, in the sense that they are “parameterized” to atomic properties, details of the simulation protocols, and especially the choice of exchange-correlation functional and whether or not empirical dispersion corrections are included, have significant impacts on the description of ion solvation and transport. For example, the bulk coordination number for OH^- is known to be dependent on the precise simulation protocol, namely, the exchange-correlation functional,^{46,47} and on dispersion corrections in slab simulations.^{55,62} Moreover, a recent study produced an empirical model of the hydroxide anion that is primarily 3-fold coordinated and gives good agreement with experimentally obtained diffusion rates.⁶⁹ The protocols used herein are similar to the ones employed in previous simulation studies of proton and negatively charged defects in water that were validated by a favorable comparison of diffusion constants and rotational relaxation times with experimental data.^{46,47} Nonetheless, more precise experimental data on the solvation structure of OH^- would be helpful for validating predictions, such as those reported here, concerning the bulk vs interfacial behavior of OH^- .

Our results also appear, at first glance, to be incompatible with surface tension data on concentrated acid and base solutions, from which positive surface excesses for acids and negative surface excesses for bases are inferred. However, we stress that our results pertain to the “intrinsic” propensities of the water ions for the air–water interface but not to finite concentrations of electrolytes, in which the effects of the presence of counterions cannot be ignored. It is important to point out that the PMFs for H_3O^+ to the air–water interface obtained by Iuchi and co-workers do sample the counterion (Cl^-) propensity.³⁵ Extensions of the aforementioned work in a pair of recent simulation studies underscore the effects of counterion on OH^- and H_3O^+ adsorption. Using a polarizable MS-EVB model that predicts a flat adsorption PMF for isolated OH^- ions,⁴⁴ Wick and Dang showed that OH^- is strongly repelled from the interface when paired with a Na^+ ion at a separation of 4 \AA .⁷⁰ Similarly, Wick found that the PMF for the isolated H_3O^+ shows no preference to or away from the air–water interface using a polarizable MS-EVB model in line with our current findings.³⁷ Upon modifying the MS-EVB model to model the interaction of the counterion with hydronium, it was found that H_3O^+ becomes more attracted to the interface when there is a Cl^- ion nearby.³⁸

Interpretation of surface tension data for acids may require, at least in some cases, a consideration of the presence of the undissociated species or associated complex (e.g., contact ion pair) at the solution–air interface that may not be present in parametrized models. For example, there is both experimental and theoretical evidence that HNO_3 is not fully dissociated in the uppermost layer of the solution–air interface,^{71–76} and that HNO_3 at aqueous interfaces behaves like HNO_3 in concentrated bulk solution.^{76,77} Thus, the existence of the molecular form at the interface should be taken into account when inferring the excesses of the ionic dissociation products from surface tension increment data.

The results presented herein suggest that both H_3O^+ and OH^- can be present at the air–water interface. Our results paint a picture in which both of the reactive self-ions of water behave like chemical defects in the hydrogen bonding network of water, in contrast to small, strongly hydrated ions such as F^- and Na^+ , which are repelled from the air–water interface. The

additional flexibility in the first solvation shell of OH^- makes it distinct from H_3O^+ . Although we cannot claim to have solved the puzzle of whether or not the water surface is enriched with protons or hydroxide ions, our work points to a fruitful avenue for future computational studies. Specifically, force field models that reproduce subtle changes of the solvation of H_3O^+ and OH^- at the interface vs bulk, such as those exposed herein, ought to be developed, validated, and applied to address issues that are currently outstanding.

AUTHOR INFORMATION

Corresponding Author

*E-mail: chris.mundy@pnnl.gov.

Notes

The authors declare no competing financial interest.

ACKNOWLEDGMENTS

D.J.T. was supported by National Science Foundation grant CHE-0909227. C.J.M. was supported by the U.S. Department of Energy's (DOE) Office of Basic Energy Sciences, Division of Chemical Sciences, Geosciences and Biosciences. Pacific Northwest National Laboratory (PNNL) is operated for the Department of Energy by Battelle. I-F.W.K. performed this work under the auspices of the U.S. Department of Energy by Lawrence Livermore National Laboratory under contract DE-AC52-07NA27344. The potential of mean force required resources of the Oak Ridge Leadership Computing Facility at the Oak Ridge National Laboratory, which is supported by the Office of Science of the U.S. Department of Energy under Contract No. DE-AC05-00OR22725. The remaining simulations and analysis used resources of the National Energy Research Scientific Computing Center, which is supported by the Office of Science of the U.S. Department of Energy under Contract No. DE-AC02-05CH11231 at Lawrence Berkeley National Laboratory. M.D.B. is grateful for the support of the Linus Pauling Distinguished Postdoctoral Fellowship Program at PNNL.

REFERENCES

- (1) Vacha, R.; Buch, V.; Milet, A.; Devlin, P.; Jungwirth, P. Autoionization at the Surface of Neat Water: is the Top Layer pH Neutral, Basic, or Acidic? *Phys. Chem. Chem. Phys.* **2007**, *9*, 4736–4747.
- (2) Petersen, P. B.; Saykally, R. J. Is the Liquid Water Surface Basic or Acidic? Macroscopic vs. Molecular-Scale Investigations. *Chem. Phys. Lett.* **2008**, *458*, 255–261.
- (3) Beattie, J. K.; Djerdjev, A. M.; Warr, G. G. The Surface of Neat Water is Basic. *Faraday Discuss.* **2009**, *141*, 31–39.
- (4) Zimmerman, R.; Freudenberg, U.; Schweiss, R.; Küttner, D.; Werner, C. Hydroxide and Hydronium Ion Adsorption – A Survey. *Curr. Opin. Colloid Interface Sci.* **2010**, *15*, 196–202.
- (5) Ben-Amotz, D. Unveiling Electron Promiscuity. *J. Phys. Chem. Lett.* **2011**, *2*, 1216–1222.
- (6) Saykally, R. J. Two Sides of the Acid-Base Story. *Nat. Chem.* **2013**, *5*, 82–84.
- (7) Washburn, E. W. *International Critical Tables of Numerical Data. Physics, Chemistry, and Technology*; McGraw-Hill: New York, 1928; Vol. IV.
- (8) Adamson, A. W.; Gast, A. P. *Physical Chemistry of Surfaces*; John Wiley and Sons: 1997.
- (9) Pegram, L. M.; Record, M. T., Jr. Quantifying Accumulation or Exclusion of H^+ , HO^- , and Hofmeister Salt Ions Near Interfaces. *Chem. Phys. Lett.* **2008**, *467*, 1–8.
- (10) Mucha, M.; Frigato, T.; Levering, L. M.; Allen, H. C.; Tobias, D. J.; Dang, L. X.; Jungwirth, P. Unified Molecular Picture of the Surfaces of Aqueous Acid, Base, and Salt Solutions. *J. Phys. Chem. B* **2005**, *109*, 7617–7623.
- (11) Petersen, P. B.; Saykally, R. J. Evidence for an Enhanced Hydronium Concentration at the Liquid Water Surface. *J. Phys. Chem. B* **2005**, *109*, 7976–7980.
- (12) Tarbuck, T. L.; Ota, S.; Richmond, G. L. Spectroscopic Studies of Solvated Hydrogen and Hydroxide Ions at Aqueous Surfaces. *J. Am. Chem. Soc.* **2006**, *128*, 14519–14527.
- (13) Levering, L. M.; Sierra-Hernandez, M. R.; Allen, H. C. Observation of Hydronium Ions at the Air-Aqueous Acid Interface: Vibrational Spectroscopic Studies of Aqueous HCl, HBr, and HI. *J. Phys. Chem. C* **2007**, *111*, 8814–8826.
- (14) Tian, C.; Ji, N.; Waychunas, G. A.; Shen, Y. R. Interfacial Structures of Acidic and Basic Solutions. *J. Am. Chem. Soc.* **2008**, *130*, 13033–13039.
- (15) Winter, B.; Faubel, M.; Vacha, R.; Jungwirth, P. Behavior of Hydroxide at the Water/Vapor Interface. *Chem. Phys. Lett.* **2009**, *474*, 241–247.
- (16) Vacha, R.; Rick, S. W.; Jungwirth, P.; de Beer, A. G. F.; de Auiar, H. B.; Samson, J.-B.; Roke, S. The Orientation and Charge of Water at the Hydrophobic Oil Droplet–Water Interface. *J. Am. Chem. Soc.* **2011**, *133*, 10204–10210.
- (17) Marinova, K. G.; Alargova, R. G.; Benkov, N. D.; Velez, O. D.; Petsev, D. N.; Ivanov, I. B.; Borwankar, R. P. Charging of Oil-Water Interfaces Due to Adsorption of Hydroxyl Ions. *Langmuir* **2006**, *12*, 2045–2051.
- (18) Beattie, J. K.; Djerdjev, A. M. The Pristine Oil/Water Interface: Surfactant-Free Hydroxide-Charged Emulsions. *Angew. Chem., Int. Ed.* **2004**, *43*, 3568–3571.
- (19) Creux, P.; Lachaise, J.; Gracia, A.; Beattie, J. K.; Djerdjev, A. M. Strong Specific Hydroxide Ion Binding at the Pristine Oil/Water and Air/Water Interfaces. *J. Phys. Chem. B* **2009**, *113*, 14146–14150.
- (20) Liu, M.; Beattie, J. K.; Gray-Weale, A. The Surface Relaxation of Water. *J. Phys. Chem. B* **2012**, *116*, 8981–8988.
- (21) Beattie, J. K.; Djerdjev, A. M.; Gray-Weale, A.; Kallay, N.; Lützenkirchen, J.; Preocanin, T.; Selmani, A. pH and the Surface Tension of Water. *J. Colloid Interface Sci.* **2014**, *422*, 54–57.
- (22) Enami, S.; Hoffman, M. R.; J, C. A. Proton Availability at the Air/Water Interface. *J. Phys. Chem. Lett.* **2010**, *1*, 1599–1604.
- (23) Mishra, H.; Enami, S.; Nielsen, R. J.; Stewart, L. A.; Hoffmann, M. R.; Goddard, W. A., III; Colussi, A. J. Bronsted Basicity of the Air-Water Interface. *Proc. Natl. Acad. Sci. U.S.A.* **2012**, *109*, 18679–18683.
- (24) Dang, L. X. Solvation of the Hydronium Ion at the Water Liquid/Vapor Interface. *J. Chem. Phys.* **2003**, *119*, 6351–6353.
- (25) Buch, V.; Milet, A.; Vacha, R.; Jungwirth, P.; Devlin, J. P. Water Surface is Acidic. *Proc. Natl. Acad. Sci. U.S.A.* **2007**, *104*, 7342–7347.
- (26) Lee, H.-S.; Tuckerman, M. E. Ab Initio Molecular Dynamics Studies of the Liquid-Vapor Interface of an HCl Solution. *J. Phys. Chem. A* **2009**, *113*, 2144–2151.
- (27) Jagoda-Cwiklik, B.; Cwiklik, L.; Jungwirth, P. Behavior of the Eigen Form of Hydronium at the Air/Water Interface. *J. Phys. Chem. A* **2011**, *115*, 5881–5886.
- (28) Ottosson, N.; Cwiklik, L.; Soderstrom, J.; Bjorneholm, O.; Ohrwall, G.; Jungwirth, P. Increased Propensity of I_{aq}^- for the Water Surface in Non-neutral Solutions: Implications for the Interfacial Behavior of H_3O^+ and OH_{aq}^- . *J. Phys. Chem. Lett.* **2011**, *2*, 972–976.
- (29) Takahashi, H.; Maruyama, K.; Karino, Y.; Morita, A.; Nakano, M.; Jungwirth, P.; Matubayasi, N. Energetic Origin of Proton Affinity to the Air/Water Interface. *J. Phys. Chem. B* **2011**, *115*, 4745–4751.
- (30) Hub, J. S.; Wolf, M. G.; Coleman, C.; van Maaren, P. J.; Groenhof, G.; van der Spoel, D. Thermodynamics of Hydronium and Hydroxide Surface Solvation. *Chem. Sci.* **2014**, *5*, 1745–1749.
- (31) Petersen, M. K.; Iyengar, S. S.; Day, T. J. F.; Voth, G. A. The Hydrated Proton at the Water Liquid/Vapor Interface. *J. Phys. Chem. B* **2004**, *108*, 14804–14806.
- (32) Iyengar, S. S.; Day, T. J. F.; Voth, G. A. On the Amphiphilic Behavior of the Hydrated Proton: an Ab Initio Molecular Dynamics Study. *Int. J. Mass Spectrom.* **2005**, *241*, 197–204.

- (33) Wang, F.; Izvekov, S.; Voth, G. A. Unusual "Amphiphilic" Association of Hydrated Protons in Strong Acid Solution. *J. Am. Chem. Soc.* **2008**, *130*, 3120–3126.
- (34) Chen, H.; Xu, J.; Voth, G. A. Unusual Hydrophobic Interactions in Acidic Aqueous Solutions. *J. Phys. Chem. B* **2009**, *113*, 7291–7297.
- (35) Iuchi, S.; Chen, H.; Paesani, F.; Voth, G. A. Hydrated Excess Proton at Water-Hydrophobic Interfaces. *J. Phys. Chem. B* **2009**, *113*, 4017–4030.
- (36) Xu, J. Q.; Izvekov, S.; Voth, G. A. Structure and Dynamics of Concentrated Hydrochloric Acid Solutions. *J. Phys. Chem. B* **2010**, *114*, 9555–9562.
- (37) Wick, C. D. Hydronium Behavior at the Air-Water Interface with a Polarizable Multistate Empirical Valence Bond Model. *J. Phys. Chem. C* **2012**, *116*, 4026–4038.
- (38) Wick, C. D. HCl Accommodation, Dissociation, and Propensity for the Surface of Water. *J. Phys. Chem. A* **2013**, *117*, 12459–12467.
- (39) Köfinger, J.; Dellago, C. Biasing the Center of Charge in Molecular Dynamics Simulations with Empirical Valence Bond Models: Free Energetics of an Excess Proton in a Water Droplet. *J. Phys. Chem. B* **2008**, *112*, 2349–2356.
- (40) Knight, C.; Voth, G. A. The Curious Case of the Hydrated Proton. *Acc. Chem. Res.* **2012**, *45*, 101–109.
- (41) Kumar, R.; Knight, C.; Voth, G. A. Exploring the Behavior of the Hydrated Excess Proton at Hydrophobic Surfaces. *Faraday Discuss.* **2013**, *167*, 263–278.
- (42) dos Santos, A. P.; Levin, Y. Surface Tensions and Surface Potentials of Acid Solutions. *J. Chem. Phys.* **2010**, *133*, 154107.
- (43) Wick, C. D.; Kuo, I.-F. W.; Mundy, C. J.; Dang, L. X. The effect of polarizability for understanding the molecular structure of aqueous interfaces. *J. Chem. Theory Comput.* **2007**, *3*, 2002–2010.
- (44) Wick, C. D.; Dang, L. X. Investigating Hydroxide Anion Interfacial Activity by Classical and Multistate Empirical Valence Bond Molecular Dynamics Simulations. *J. Phys. Chem. A* **2009**, *113*, 6356–6364.
- (45) Wick, C. D.; Dang, L. X. The Behavior of NaOH at the Air-Water Interface: A Computational Study. *J. Chem. Phys.* **2010**, *133*.
- (46) Tuckerman, M. E.; Chandra, A.; Marx, D. Structure and Dynamics of OH[−](aq). *Acc. Chem. Res.* **2006**, *39*, 151–158.
- (47) Marx, D.; Chandra, A.; Tuckerman, M. E. Aqueous Basic Solutions: Hydroxide Solvation, Structural Diffusion, and Comparison to the Hydrated Proton. *Chem. Rev.* **2010**, *110*, 2174–2216.
- (48) Fulton, J. L.; Schenter, G. K.; Baer, M. D.; Mundy, C. J.; Dang, L. X.; Balasubramanian, M. Probing the Hydration Structure of Polarizable Halides: A Multiedge XAFS and Molecular Dynamics Study of the Iodide Anion. *J. Phys. Chem. B* **2010**, *114*, 12926–12937.
- (49) Baer, M. D.; Pham, V.-T.; Fulton, J. L.; Schenter, G. K.; Balasubramanian, M.; Mundy, C. J. Is Iodate a Strongly Hydrated Cation? *J. Phys. Chem. Lett.* **2011**, *2*, 2650–2654.
- (50) Baer, M. D.; Mundy, C. J. An Ab Initio Approach to Understanding the Specific Ion Effect. *Faraday Discuss.* **2013**, *160*, 89–101.
- (51) Geissler, P. L. Water Interfaces, Solvation, and Spectroscopy. *Annu. Rev. Phys. Chem.* **2013**, *64*, 317–337.
- (52) Tobias, D. J.; Stern, A. C.; Baer, M. D.; Levin, Y.; Mundy, C. J. Simulation and Theory of Ions at Atmospherically Relevant Aqueous Liquid-Air Interfaces. *Annu. Rev. Phys. Chem.* **2013**, *64*, 339–359.
- (53) Jungwirth, P. Spiers Memorial Lecture: Ions at Aqueous Interfaces. *Faraday Discuss.* **2009**, *141*, 9–30.
- (54) Kudin, K. N.; Car, R. Why Are Water–Hydrophobic Interfaces Charged? *J. Am. Chem. Soc.* **2008**, *130*, 3916–3919.
- (55) Mundy, C. J.; Kuo, I.-F. W.; Tuckerman, M. E.; Lee, H.-S.; Tobias, D. J. Hydroxide Anion at the Air-Water Interface. *Chem. Phys. Lett.* **2009**, *481*, 2–8.
- (56) VandeVondele, J.; Krack, M.; Mohamed, F.; Parrinello, M.; Chassaing, T.; Hutter, J. QUICKSTEP: Fast and Accurate Density Functional Calculations using a Mixed Gaussian and Plane Waves Approach. *Comput. Phys. Commun.* **2005**, *167*, 103–128.
- (57) Goedecker, S.; Teter, M.; Hutter, J. Separable Dual-Space Gaussian Pseudopotentials. *Phys. Rev. B* **1996**, *54*, 1703–1710.
- (58) Grimme, S. Accurate Description of Van der Waals Complexes by Density Functional Theory Including Empirical Corrections. *J. Comput. Chem.* **2004**, *25*, 1463–1473.
- (59) Becke, A. D. Density-Functional Exchange-Energy Approximation with Dorrect Asymptotic Behavior. *Phys. Rev. A* **1988**, *38*, 3098–3100.
- (60) Lee, C.; Yang, W.; Parr, R. G. Development of the Colle-Salvetti Correlation-Energy Formula into a Functional of the Electron Density. *Phys. Rev. B* **1988**, *37*, 785–789.
- (61) Martyna, G. J.; Klein, M. L.; Tuckerman, M. E. Nose-Hoover Chains - The Canonical Ensemble via Continuous Dynamics. *J. Chem. Phys.* **1992**, *97*, 2635–2643.
- (62) Baer, M. D.; Mundy, C. J.; McGrath, M. J.; Kuo, I. F. W.; Siepmann, J. I.; Tobias, D. J. Re-examining the Properties of the Aqueous Vapor-Liquid Interface Using Dispersion Corrected Density Functional Theory. *J. Chem. Phys.* **2011**, *135*.
- (63) Marx, D.; Tuckerman, M. E.; Hütter, J.; Parrinello, M. The Nature of the Excess Proton in Water. *Nature* **1999**, *397*, 601–604.
- (64) VandeVondele, J.; Hutter, J. Gaussian Basis Sets for Accurate Calculations on Molecular Systems in Gas and Condensed Phases. *J. Chem. Phys.* **2007**, *127*, 114105.
- (65) Robertson, W. H.; Diken, E. G.; Price, E. A.; Shin, J.-W.; Johnson, M. A. Spectroscopic Determination of the OH[−] Solvation Shell in the OH-(H₂O)_n Clusters. *Science* **2003**, *299*, 1367–1372.
- (66) Kuo, I.-F. W.; Mundy, C. J. An Ab Initio Molecular Dynamics Study of the Aqueous Liquid-Vapor Interface. *Science* **2004**, *303*, 658–660.
- (67) Ho, M.-H.; Klein, M. L.; Kuo, I.-F. W. Bulk and Interfacial Aqueous Fluoride: An Investigation via First Principles Molecular Dynamics. *J. Phys. Chem. A* **2009**, *113*, 2070–2074.
- (68) Pluharova, E.; Marsalek, O.; Schmidt, B.; Jungwirth, P. Ab Initio Molecular Dynamics Approach to a Quantitative Description of Ion Pairing in Water. *J. Phys. Chem. Lett.* **2013**, *4*, 4177–4181.
- (69) Kale, S.; Herzfeld, J. Proton Defect Solvation and Dynamics in Aqueous Acid and Base. *Angew. Chem., Int. Ed.* **2012**, *51*, 11029–11032.
- (70) Cummings, O. T.; Wick, C. D. Computational study of cation influence on anion propensity for the air-water interface. *Chem. Phys. Lett.* **2010**, *500*, 41–45.
- (71) Schnitzer, C.; Baldelli, S.; Campbell, D. J.; Schultz, M. J. Sum Frequency Generation of O–H Vibrations on the Surface of H₂O/HNO₃ Solutions and Liquid HNO₃. *J. Phys. Chem. A* **1999**, *103*, 6383–6386.
- (72) Donaldson, D. J.; Anderson, D. Does Molecular HNO₃ Adsorb Onto Sulfuric Acid Droplet Surfaces? *Geophys. Res. Lett.* **1999**, *26*, 3625–3628.
- (73) Soule, M. C. K.; Blower, P. G.; Richmond, G. L. Nonlinear Vibrational Spectroscopic Studies of the Adsorption and Speciation of Nitric Acid at the Vapor/Acid Solution Interface. *J. Phys. Chem. A* **2007**, *111*, 3349–3357.
- (74) Shamay, E. S.; Buch, V.; Parrinello, M.; Richmond, G. L. At the Water's Edge: Nitric Acid as a Weak Acid. *J. Am. Chem. Soc.* **2007**, *129*, 12910–12911.
- (75) Wang, S.; Bianco, R.; Hynes, J. T. Depth-Dependent Dissociation of Nitric Acid at an Aqueous Surface: Car-Parrinello Molecular Dynamics. *J. Phys. Chem. A* **2003**, *113*, 1295–1307.
- (76) Lewis, T.; Winter, B.; Stern, A. C.; Baer, M. D.; Mundy, C. J.; Tobias, D. J.; Hemminger, J. C. Does Nitric Acid Dissociate at the Aqueous Solution Surface? *J. Phys. Chem. C* **2011**, *115*, 21183–21190.
- (77) Lewis, T.; Winter, B.; Stern, A. C.; Baer, M. D.; Mundy, C. J.; Tobias, D. J.; Hemminger, J. C. Dissociation of Strong Acid Revisited: X-ray Photoelectron Spectroscopy and Molecular Dynamics Simulations of HNO₃ in Water. *J. Phys. Chem. B* **2011**, *115*, 9445–9451.